BMC Chemistry

RESEARCH

Open Access

Removal of Pb(II) ions by cellulose modified-$LaFeO_3$ sorbents from different biomasses

Shimaa M. Ali[1*], Mohamed A. El Mansop[1], Ahmed Galal[1], Soha M. Abd El Wahab[2], Wafaa M. T. El-Etr[3] and Hanaa A. Zein El-Abdeen[3]

Abstract

$LaFeO_3$ perovskite is prepared by the cellulose-modified microwave-assisted citrate method using two different biomasses as a cellulose source; rice straw (RS) and banana peel (BP). The prepared samples are assigned as $LaFeO_3$/cellulose-RS and as $LaFeO_3$/cellulose-BP, respectively. Raman Spectra prove the presence of perovskite and cellulose phases, as well as biochar resulted from the thermal treatment of the cellulose. $LaFeO_3$/cellulose-RS has a cauliflower morphology while, two phases are observed for $LaFeO_3$/cellulose-BP, mesoporous cellulose phase and octahedral $LaFeO_3$ nanoparticles as shown by scanning electron microscope (SEM) images. $LaFeO_3$/cellulose-BP has higher porosity and larger BET surface area than $LaFeO_3$/cellulose-RS. Both samples are applied for the removal of Pb(II) ions from aqueous solution by adsorption. The adsorption follows Langmuir isotherm, with maximum adsorption capacities of 524 and 730 mg/g for $LaFeO_3$/cellulose-RS and $LaFeO_3$/cellulose-BP, respectively. Cellulose precursors from different biomasses affect structural and morphological properties of $LaFeO_3$/cellulose samples as well as the sorption performance for Pb(II) ions. BP is more recommended than RS, as a biomass, in the present study.

Keywords $LaFeO_3$ perovskite, Cellulose-modified synthesis method, Biomass type, Adsorption, Water decontamination

Introduction

A considerable amount of toxic Pb(II) ion is released to the environment and pollutes water as an industrial effluent of many processes such as battery and chemicals manufacture, refining, and automobile maintenance [1]. Pb(II) ion is toxic and has the most global abundance among heavy metal ions [2]. It accumulates in the human body, causing dangerous diseases such as, kidneys and brain damage, anemia, cancer, and many others [3]. The removal of Pb(II) ions, and other toxic metal ions, from wastewater is an essential and critical issue [4, 5]. There are several methods that can be applied for example, adsorption [6], coagulation [7], membrane filtration [8], chemical precipitation [9], electrodialysis [10], etc. The method used in this work is adsorption, not only because it is simple and cost-effective method but also, due to the progress in materials science, which permits researchers to prepare novel and efficient sorbents materials. An economically trend, that has been recently and extensively applied, is the use of waste for waste, i.e. the use of agricultural waste or biomass to prepare sorbents for the removal of toxic pollutants from wastewater. Due to simplicity, availability, and low cost, raw and modified

*Correspondence:
Shimaa M. Ali
Sali@sci.cu.edu.eg
[1] Chemistry Department, Faculty of Science, Cairo University, Giza 12613, Egypt
[2] Physics Department, Faculty of Science, Cairo University, Giza 12613, Egypt
[3] Soil, Water and Environmental Research Institute, Agriculture Research Center (ARC), Giza 12613, Egypt

biomasses are highly recommended as efficient sorbents, for example, Banana and orange peels, rice straw, potato, cucumber, watermelon and tea waste [11]. A modification or a pretreatment step of the cellulose-containing agricultural waste is advisable in sorption applications, to enrich the functional groups and increase the surface area and porosity [12]. The pretreatment step can be performed by several ways such as alkalization [13], acidification [14], esterification [15], etherification [16], carbonization [17], magnetization [18], and grafting [19]. The performance is expected to be better by using composites of the biomass with nanomaterials.

Perovskites nanomaterials are mixed metal oxides of the general formula ABO_3, where A is a lanthanide and B is a transition metal. Due to the highly stabilized B metal in the perovskite matrix, perovskites possess many interesting structural, electrical, magnetic, optical properties [20–22]. Perovskites are highly recommended candidates in several important application, such as catalysis [23], sensors [24], capacitors [25], energy-storage [26], optical [27], and electrical devices [28], etc. The use of perovskites as sorbents for the removal of organic and inorganic pollutants is recently, but not too many, reported [29–31]. In our previous work, we used lanthanum-iron based-perovskite, prepared by the cellulose-modified method, for the removal of organic congo red dye [32], and inorganic toxic heavy metal ions; Pb(II), Cd(II), and Cu(II) ions [33]. The cellulose-modified method is performed by adding a raw or modified agricultural waste containing cellulose during the early stage of the perovskite synthesis. The product is perovskite-cellulose/biochar composite, rather than a pure perovskite [32].

In this work, $LaFeO_3$ perovskite is prepared by the cellulose-modified microwave-assisted citrate method using two types of pretreated biomasses; rice straw (RS) and banana peel (BP). The effect of changing the biomass type on structural and surface properties of the prepared materials; $LaFeO_3$/cellulose-RS and as $LaFeO_3$/cellulose-BP are examined. Both samples are applied as sorbents for the removal of Pb(II) ion, the effect of the pretreatment step as well as changing the biomass type on the adsorption efficiency is investigated. The possibility of the sorbent regeneration and reuse, as well as, the performance in the real sample is studied.

Experimental

Chemicals

Ferric nitrate nonahydrate (98%), lanthanum (III) nitrate hexahydrate (99%), citric acid (98%), nitric acid (69%), acetic acid glacial ≥99%, ammonium hydroxide solution (30–33%), sodium hydroxide ≥98%, sodium chlorite (80%), lead nitrate (99%), cadmium chloride hydrate (98%), and copper sulfate pentahydrate (98%) are bought from Sigma-Aldrich. Bromocresol green is bought from Qualikems.

Pretreatment of biomass

Cellulose is isolated by pretreatment of two different biomasses, rice straw (RS) and banana peel (BP) as reported [34]. Briefly, biomass is washed, dried, and grounded into a powder. The biomass powder is heated with 12 wt% of NaOH at 120 °C for 1 h to purify cellulose from lignin and hemicellulose. The solution is centrifuged and washed with distilled water. The residual is dried and added to acidified 5 wt% sodium chlorite at 75 °C for 90 min. The residual, α-cellulose, is washed with distilled water and dried at 40 °C overnight.

Synthesis of $LaFeO_3$ by the cellulose-modified citrate microwave-assisted method

Ferric nitrate nonahydrate and lanthanum (III) nitrate hexahydrate are weighed in an equal molar ratio and dissolved in distilled water. Cellulose from either RS or BP is added to the mixed metals ions solution, and shaken for 24 h. The pH value is adjusted at 8 by 1 mmol L^{-1} nitric acid and 1mmol/L^{-1} ammonia solution, then citric acid is added in a molar amount equals to the total molar amount of metal ions. The mixed complex/cellulose suspension is heated till evaporation then placed in the microwave oven (720 W) for 30 min (20-s on and 10-s off). After dryness, the residual is ignited and finally calcinated at 450 °C for 3 h to obtain $LaFeO_3$/cellulose-RS and $LaFeO_3$/cellulose-BP materials [32, 33].

Adsorption experiment

50 mg of $LaFeO_3$/cellulose material is added to 25 mL of Pb(II) ion solution with an adjusted pH value at 7. The solution is shaken for 24 h, then it is filtered through 0.45 µm nylon syringe filter. The concentration of unadsorbed Pb(II) ions is determined by the atomic absorption spectroscopy (NovAA 350).

The removal % and the amount of adsorbed Pb(II) ions, q_e, are determined from Eqs. (1) and (2), respectively [35]:

$$Removal\,\% = \frac{C_o - C_e}{C_o} \times 100 \tag{1}$$

$$q_e = \frac{C_{ads \times V_L}}{m} \tag{2}$$

where, C_o, C_e, and C_{ads} are initial, remaining, and adsorbed concentrations of Pb(II) ions (mg/g), respectively. V_L is the volume of the solution (L), and m is the mass of the adsorbent (g).

Characterization techniques

Raman spectroscopy, Horiba labRAM HR evolution visible single spectrometer is used for structural identification. The particle size distribution is determined by the zeta seizer instrument (NanoSight NS500, Malvern Panalytical) by dynamic light scattering (DLS) method. Scanning electron microscope (SEM), (JEOL JXA-840A) is used for the morphological characterization. Brunauer–Emmett–Teller (BET) surface area is calculated using N_2 gas as an adsorbate at 77 K, and done by Nova Touch, Quanta Chrome.

Results and discussion

Structural and surface characterizations

Raman spectroscopy

Raman spectroscopy is used for the structure identification of prepared samples, Fig. 1 shows Raman spectra of $LaFeO_3$/cellulose-RS (A), and $LaFeO_3$/cellulose-BP (B). The formation of the octahedral $LaFeO_3$ perovskite phase is ascertained by the appearance of bands at 292, 415, and 686 cm^{-1}, which correspond to oxygen octahedral tilt, bending, and stretching vibration, respectively [36]. Characteristic cellulose bands are located around 1030 cm^{-1}, and are assigned for symmetric and asymmetric stretching vibration of β-(1,4)-glycosidic linkage. Bands located at 1390 and 2896 cm^{-1} are assigned for CH_2 bending and stretching modes, respectively [37]. The intensities of these band can be correlated to the crystallinity arrangement as well as the cellulose chain length. It can be noticed that cellulose sample prepared by using banana peel shows a longer chain length and a comparable crystallinity to that prepared by using straw rice. The appearance of the biochar phase, due to the thermal treatment of cellulose, is also detected by bands located at 1260 cm^{-1}, 1502 cm^{-1}, and band located between 2400 to 3050 cm^{-1}. These bands correspond to D-, G-, and 2D-bands, respectively [38].

Scanning electron microscope (SEM) and particle size distribution

Figure 2 shows SEM images of $LaFeO_3$/cellulose-RS (A), and $LaFeO_3$/cellulose-BP (B). The insets represent the corresponding particle size distribution, estimated by DLS method. $LaFeO_3$/cellulose-RS has a cauliflower-like morphology, Fig. 2A. While $LaFeO_3$/cellulose-BP has a different morphology, in which two phases can be assigned; mesoporous phase of cellulose and biochar, and nanoparticle of octahedral $LaFeO_3$ perovskite, Fig. 2B. The average particle size values are 32 and 38 nm for $LaFeO_3$/cellulose-RS and $LaFeO_3$/cellulose-BP, respectively, insets of Fig. 2.

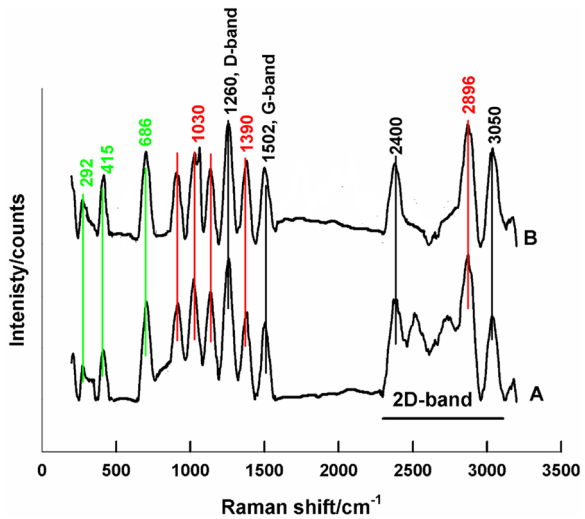

Fig. 1 Raman spectra of $LaFeO_3$/cellulose-RS (**A**), and $LaFeO_3$/cellulose-BP (**B**)

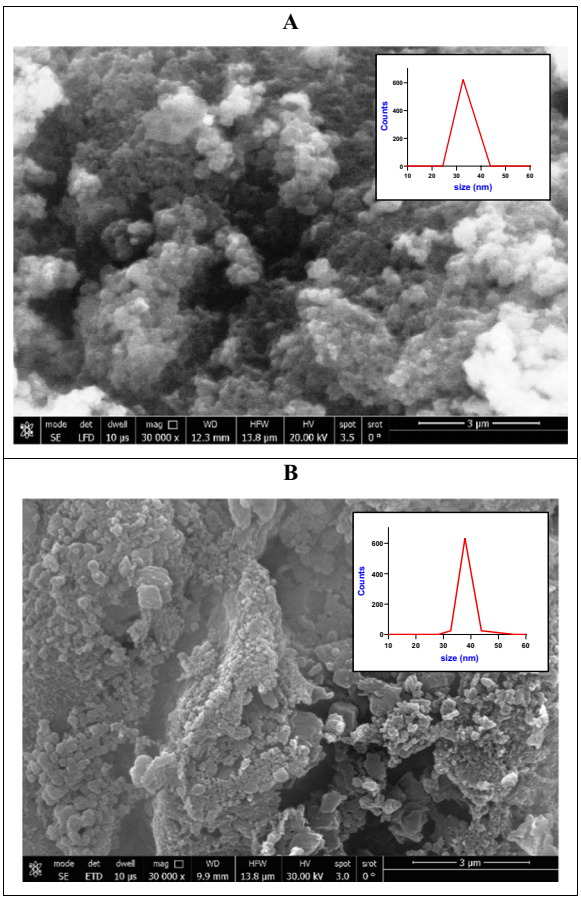

Fig. 2 SEM images of $LaFeO_3$/cellulose-RS (**A**), and $LaFeO_3$/cellulose-BP (**B**). The insets are the corresponding particle size distribution, estimated by DLS method

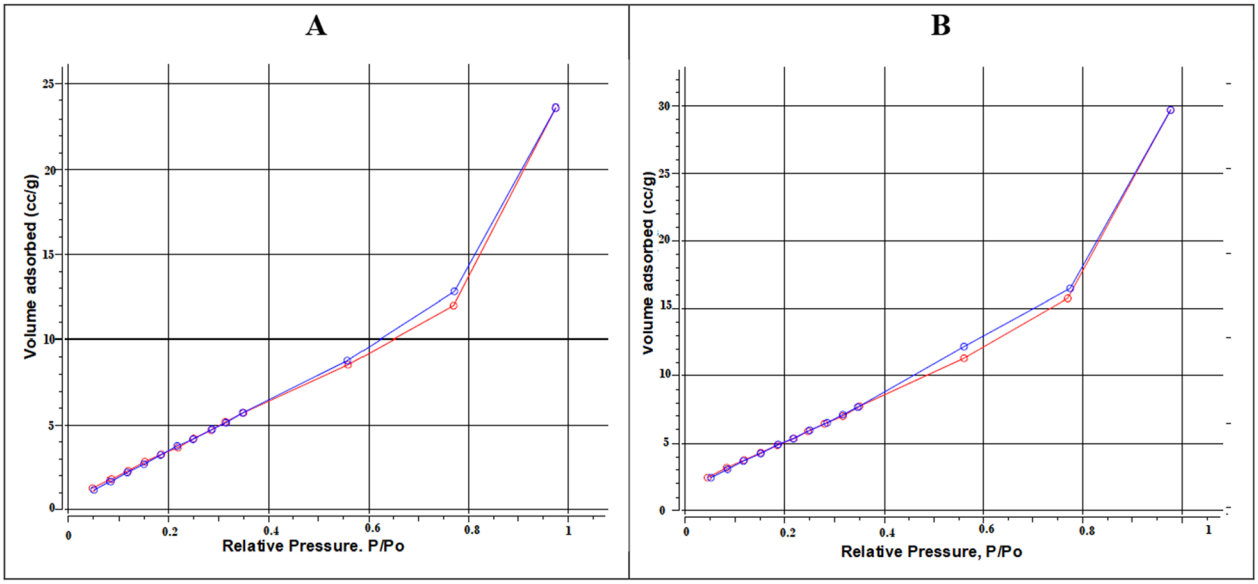

Fig. 3 BET hysteresis loops for nitrogen adsorption/desorption on $LaFeO_3$/cellulose-RS (**A**), and $LaFeO_3$/cellulose-BP (**B**)

Table 1 Average pore size and volume as well as measured surface area calculated by BET method for the prepared samples

Sample	BET surface m^2/g	Total pore volume (cc/g)	Average pore size (nm)
$LaFeO_3$/cellulose-RS	20.99	0.0366	3.49
$LaFeO_3$/cellulose-BP	24.58	0.0460	3.74

BET surface area measurements

Nitrogen adsorption/desorption hysteresis loops for the prepared samples are shown in Fig. 3. Both loops are H3 types, which means that both samples; $LaFeO_3$/cellulose-RS, and $LaFeO_3$/cellulose-BP have pores of a slit-like shape [39, 40]. The pore size and pore volume as well as the surface area are calculated by the BET method and listed in Table 1. It can be shown $LaFeO_3$/cellulose-RS sample has smaller pore size and pore volume than $LaFeO_3$/cellulose-BP sample, which indicated the decreased sample porosity by using cellulose prepared from RS. The calculated BET surface areas are 20.99 and 24.58 m^2/g for $LaFeO_3$/cellulose-RS and $LaFeO_3$/cellulose-BP, respectively. According to the particle size distribution profiles of the two samples, insets of Fig. 2, $LaFeO_3$/cellulose-RS sample has a smaller particle size of 32 nm as compared to that of $LaFeO_3$/cellulose-BP sample, 38 nm. It can be concluded that the former has a lower porosity as indicated by its smaller particle size and decreased surface area with respect to the banana peel-based perovskite sample.

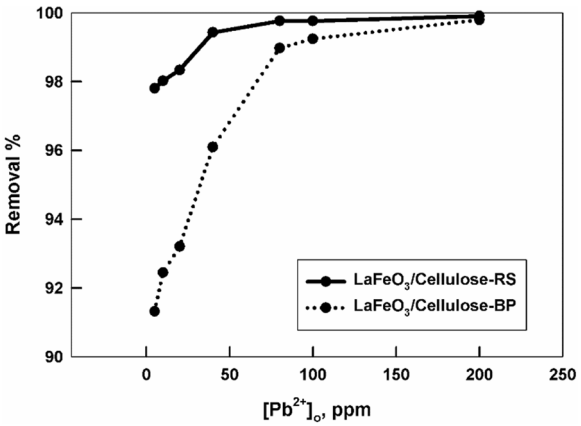

Fig. 4 The variation of the removal % of $LaFeO_3$/cellulose-RS and $LaFeO_3$/cellulose-BP for Pb(II) ions at pH = 7 for a shaking time = 2 h at room temperature

Application of cellulose-modified $LaFeO_3$ samples as sorbents for the removal of Pb(II) ions from aqueous solutions

Effect of the initial Pb(II) ion concentration

The adsorption experiments of Pb(II) ion on each of the prepared samples, $LaFeO_3$/cellulose-RS, and $LaFeO_3$/cellulose-BP, are conducted at different initial Pb(II) ion concentration, ranging from 5 to 200 ppm, at pH = 7 and room temperature. Figure 4 shows the dependence of the removal % of Pb(II) ions by perovskite/cellulose samples on the initial metal ion concentration. The removal % is high, > 90% and increases with increasing the initial

metal ion concentration, which indicates the availability of active adsorption sites [41]. $LaFeO_3$/cellulose-RS offers a better removal performance for Pb(II) ions at low initial metal ion concentration with respect to $LaFeO_3$/cellulose-BP, while at high concentration ≥100 ppm, both samples exhibit a comparable sorption ability.

Adsorption isotherms

For a better elucidation of the adsorption mechanism, the adsorption data of Pb(II) ions, on perovskites samples modified with cellulose from different biomasses; RS and BP, are fitted to different isotherms; Langmuir, Freundlich, and Temkin isotherms. While Langmuir and Freundlich isotherms suppose that there is no lateral interaction, Temkin isotherm assumes the existence of adsorbate-sorbent interaction. Linear forms of Langmuir, Freundlich, and Temkin isotherms can be expressed by the following equations, respectively [42]:

$$\frac{1}{q_e} = \frac{1}{q_m} + \frac{1}{q_m K_L C_e} \tag{3}$$

$$ln\ q_e = ln\ K_F + \frac{1}{n}\ ln\ C_e \tag{4}$$

$$q_e = \frac{RT}{b} lnK_T + \frac{RT}{b} \ln C_e \tag{5}$$

where q_m is the maximum adsorption capacity (mg/g), K_L, (. K_F and n), and (K_T and b) are Langmuir, Freundlich, and Temkin constants, respectively. Figure 5 shows the different adsorption isotherms for the adsorption of Pb(II) ions on perovskites samples modified with cellulose prepared from RS and BP. Table 2 summarizes the calculated parameters from the different isotherms for the adsorption of Pb(II) ions on the two proposed sorbents.

Based on the correlation coefficient, r^2, values, the adsorption data fits better Langmuir isotherm for both, $LaFeO_3$/cellulose-RS and $LaFeO_3$/cellulose-BP. This means that the adsorption of Pb(II) ions on perovskite modified-cellulose samples is a monolayer adsorption in which adsorbed Pb(II) ions form coordination bonds with the functional groups at the sorbent surface [43]. The same mechanism is verified, irrespective to the biomass type used as a source for the cellulose precursor. However, the calculated maximum adsorption capacities, q_m, are 523.6 and 729.9 mg/g for $LaFeO_3$/cellulose-RS and $LaFeO_3$/cellulose-BP, respectively. BP is more recommended as a biomass for cellulose preparation in this work. This is due to longer chains, and increased porosity and surface area offered by $LaFeO_3$/cellulose-BP as compared to $LaFeO_3$/cellulose-RS. It was reported that the adsorption of Pb(II) ions on biochar prepared from RS is based on chemical complexation mechanism with q_m value of 176.1 mg/g [44], while for biochar prepared from BP, the q_m value is 247.1 mg/g [45]. This finding agrees well with the sorption performance reported in this work. In a previous work, we used BP during the perovskite synthesis without the pretreatment step [32]. The calculated q_m value for the adsorption of Pb(II) ions, is 606.1 mg/g, which is smaller than that reported in this work. Therefore, it is recommended to perform the pretreatment step of the biomass before the perovskite synthesis.

Regeneration and reuse

The possibility of the sorbent regeneration and reuse for the remove of Pb(II) ions are checked for the two prepared samples $LaFeO_3$/cellulose-RS and $LaFeO_3$/cellulose-BP. Sorbents are regenerated by being shaken in 1% HNO_3 solution for 24 h, then samples are washed with distilled water and dried at 40 °C for 24 h, before reuse [32]. Figure 6A shows the variation of the removal % of Pb(II) ions by $LaFeO_3$/cellulose-RS and $LaFeO_3$/cellulose-BP, with repeated regeneration and reuse cycles.

Both sorbents can be regenerated and reused successively for 3 cycles, the decrease of the removal % by performing three successive usage cycles are 3.6 and 2.3% for $LaFeO_3$/cellulose-RS and $LaFeO_3$/cellulose-BP, respectively. Starting from the 4th cycle, the sorption efficiency is decreased to about 20%, of the value calculated for the fresh $LaFeO_3$/cellulose-RS sample, and decreased to about 40% of the value calculated for the fresh $LaFeO_3$/cellulose-BP sample. This reflects that the latter is a better sorbent. The decrease in the adsorption ability by successive cycles of adsorption and desorption can be due to the accumulation of impurities or contaminants on the surface that block the active sites or pores of the adsorbent or the degradation or deterioration of the adsorbent structure due to thermal, chemical, or mechanical stress.

Interferences study

The sorption performance of $LaFeO_3$/cellulose-RS and $LaFeO_3$/cellulose-BP for Pb(II) ion is checked firstly, in the presence of other heavy metal ions; 30 ppm Cu(II) and 30 ppm Cd(II) ions, as inorganic pollutants. Secondly, in the presence of 30 ppm bromocresol green dye, as an organic pollutant. The removal % of the two proposed sorbents, for Pb(II) ion, is compared for the three cases; when Pb(II) ions present individually, in the presence of inorganic pollutants, and in the presence of organic pollutants, as shown in Fig. 6B. The removal % of $LaFeO_3$/cellulose-RS for Pb(II) ions is slightly decreased by the presence of inorganic and organic pollutants (decreased by about 3% as compared to the individual case). While,

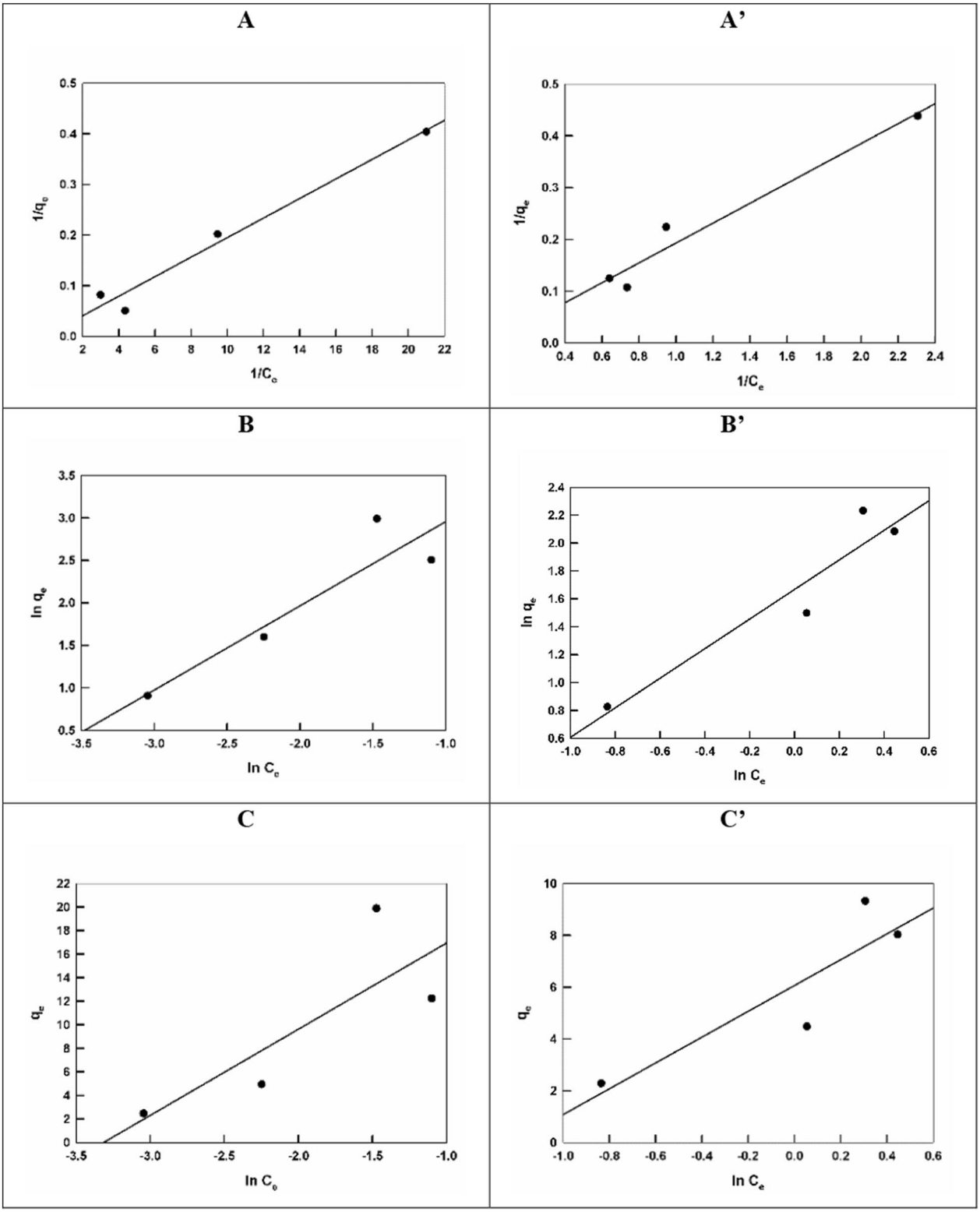

Fig. 5 Langmuir (**A**, **A**'), Freundlich (**B**, **B**'), and Temkin (**C**, **C**') isotherms for the adsorption of Pb(II) ions of $LaFeO_3$/cellulose-RS and $LaFeO_3$/cellulose-BP, respectively

Table 2 Adsorption parameters calculated by fitting Langmuir, Freundlich, and Temkin isotherms to the adsorption data of Pb(II) ions on $LaFeO_3$/cellulose-RS and $LaFeO_3$/cellulose-BP

Sorbent	Langmuir isotherm			Freundlich isotherm			Temkin isotherm		
	q_m (mg/g)	K_L (L/mg)	r^2	n	K_F ($mg^{1-(1/n)} L^{1/n}/g$)	r^2	b (kJ/mol)	K_T (L/mg)	r^2
$LaFeO_3$/cellulose-RS	523.56	0.096	0.9730	1.01	51.94	0.8487	338.82	27.94	0.6469
$LaFeO_3$/cellulose-BP	729.93	0.007	0.9580	0.94	5.31	0.9072	496.67	3.39	0.7871

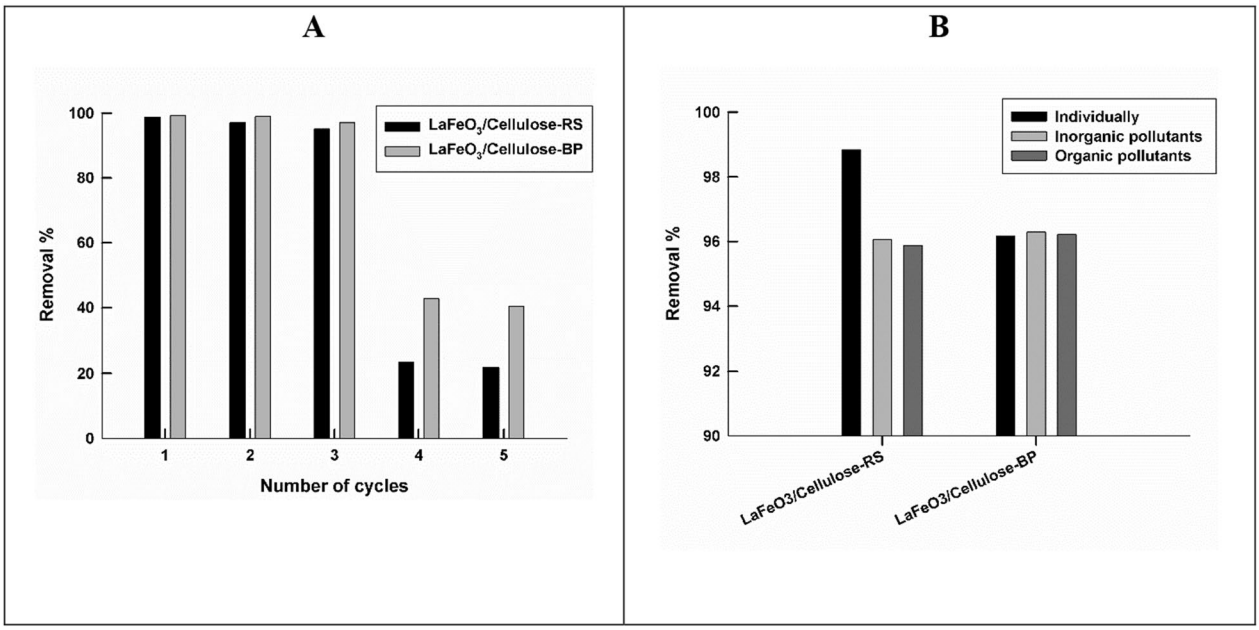

Fig. 6 The variation of the removal % of Pb(II) ions by $LaFeO_3$/cellulose-RS and $LaFeO_3$/cellulose-BP, with successive regeneration and reuse cycles (**A**), In the absence and presence of inorganic or organic pollutants (**B**)

The removal % of $LaFeO_3$/cellulose-BP for Pb(II) ions is not affected by the presence of inorganic and organic pollutants. Therefore, both sorbents can be used effectively for the removal of Pb(II) ions without being affected by the matrix of the real sample, and highly recommended for the field applications.

Conclusion

- $LaFeO_3$ perovskite can be successively prepared by the cellulose-modified microwave-assisted citrate method. The product is a composite of $LaFeO_3$, cellulose, and biochar, as confirmed by Raman spectroscopy. The appearance of oxygen octahedral bands, vibration of β-(1,4)-glycosidic linkage, and D-, G-, and 2D-bands, respectively.
- Changing the biomass used as a cellulose source, either RS or BP, affect the structure, morphology, and surface area of the prepared perovskite. $LaFeO_3$/cellulose-RS (20.99 m^2/g) has a cauliflower-like morphology, while $LaFeO_3$/cellulose-BP (24.58 m^2/g) has two phases; mesoporous cellulose and biochar, and perovskite nanoparticles.
- The prepared $LaFeO_3$/cellulose-RS and $LaFeO_3$/cellulose-BP are applied as sorbents for the removal of Pb(II) ions from aqueous solution. Adsorption follows Langmuir isotherm, and calculated q_m values are 523.6 and 729.9 mg/g for $LaFeO_3$/cellulose-RS and $LaFeO_3$/cellulose-BP, respectively.
- Proposed sorbents can be effectively regenerated and reused for successive three cycles, and can perform efficiently in the real sample matrix.
- Both sorbents exhibit an excellent sorption performance with a preferred direction to use of BP as a cellulose source during the sorbent synthesis due to the better adsorption efficiency and higher selectivity.

Acknowledgements
Not applicable.

Author contributions
SMA: methodology, analysis, data interpretation, supervision, writing the original draft. MAE: contributed to methodology. AG: supervision, editing. SMAW: contributed to methodology, supervision editing. WMTE: supervision, editing. HAZ: contributed to methodology, supervision, editing. All authors read and approved the final manuscript.

Funding
Open access funding provided by The Science, Technology & Innovation Funding Authority (STDF) in cooperation with The Egyptian Knowledge Bank (EKB).

Availability of data and materials
The data and materials of this research are available by requesting from the corresponding author.

Declarations

Ethics approval and consent to participate
Not applicable.

Consent for publication
Not applicable.

Competing interests
There are no competing interests reported by authors.

Received: 12 July 2023 Accepted: 26 October 2023
Published online: 04 November 2023

References

1. Hashem A, Fletcher A, Younis H, Mauof H, Abou-Okeil A. Adsorption of Pb (II) ions from contaminated water by 1,2,3,4-butanetetracarboxylic acid-modified microcrystalline cellulose: Isotherms, kinetics, and thermodynamic studies. Int J Biol Macromol. 2020;164:3193–203.
2. Xie Y, Yuan X, Wu Z, Zeng G, Jiang L, Peng X, et al. Adsorption behavior and mechanism of Mg/Fe layered double hydroxide with Fe_3O_4-carbon spheres on the removal of Pb (II) and Cu (II). J Colloid Interface Sci. 2019;536:440–55.
3. Qu J, Meng Q, Lin X, Han W, Jiang Q, Wang L, et al. Microwave-assisted synthesis of betacyclodextrin functionalized celluloses for enhanced removal of Pb (II) from water: Adsorptive performance and mechanism exploration. Sci Total Environ. 2020;752: 141854.
4. Modak A, Das S, Chanda D, Samanta A, Jana S. Thiophene containing microporous and mesoporous nanoplates for separation of mercury from aqueous solution. N J Chem. 2019;43:3341–9.
5. Modak A, Bhanja P, Selvaraj M, Bhaumik A. Functionalized porous organic materials as efficient media for the adsorptive removal of Hg(II) ions. Environ Sci Nano. 2020;7:2887–923.
6. Ali SM. Fabrication of a nanocomposite from an agricultural waste and its application as a biosorbent for organic pollutants. Int J Environ Sci Tech. 2018;15:1169–78.
7. Pang FM, Kumar P, Teng TT, Omar AKM, Wasewar KL. Removal of lead, zinc and iron by coagulation–flocculation. J Taiwan Inst Chem Eng. 2011;42:809–15.
8. Huang L, Wu B, Wu Y, Yang Z, Yuan T, Alhassan SI, et al. Porous and flexible membrane derived from ZIF-8-decorated hyphae for outstanding adsorption of Pb^{2+} ion. J Colloid Interface Sci. 2020;565:465–73.
9. Nemeth G, Mlinárik L, Török Á. Adsorption and chemical precipitation of lead and zinc from contaminated solutions in porous rocks: possible application in environmental protection. J Afr Earth Sci. 2016;122:98–106.
10. Al-Shannag M, Al-Qodah Z, Bani-Melhem K, Qtaishat MR, Alkasrawi M. Heavy metal ions removal from metal plating wastewater using electrocoagulation: kinetic study and process performance. Chem Eng J. 2015;260:749–56.
11. Anastopoulos I, Pashalidis I, Hosseini-andegharaei A, Giannakoudakis DA, Robalds A, Usman M, et al. Agricultural biomass/waste as adsorbents for toxic metal decontamination of aqueous solutions. J Mol Liq. 2019;295: 111684.
12. Liu G, Dai Z, Liu X, Dahlgren RA, Xu J. Modification of agricultural wastes to improve sorption capacities for pollutant removal from water. Carbon Res. 2022;1:24.
13. Kovacova Z, Demcak S, Balintova M, Pla C, Zinicovscaia I. Influence of wooden sawdust treatments on Cu(II) and Zn(II) removal from water. Materials. 2020;13:3575.
14. Yanyan L, Kurniawan TA, Zhu M, Ouyang T, Avtar R, Othman MHD, et al. Removal of acetaminophen from synthetic wastewater in a fixed-bed column adsorption using low-cost coconut shell waste pretreated with NaOH, HNO_3, ozone, and/or chitosan. J Environ Manag. 2018;226:365–76.
15. Pang L, Gao Z, Feng H, Wang S, Wang Q. Cellulose based materials for controlled release formulations of agrochemicals: a review of modifications and applications. J Control Release. 2019;316:105–15.
16. Kong W, Li Q, Li X, Su Y, Yue Q, Zhou W, et al. Removal of copper ions from aqueous solutions by adsorption onto wheat straw cellulosebased polymeric composites. J Appl Polym Sci. 2018;135:4668036.
17. Yang X, Wan Y, Zheng Y, He F, Yu Z, Huang J, et al. Surface functional groups of carbon-based adsorbents and their roles in the removal of heavy metals from aqueous solutions: a critical review. Chem Eng J. 2019;366:608–21.
18. Shao Y, Gao Y, Yue Q, Kong W, Gao B, Wang W, et al. Degradation of chlortetracycline with simultaneous removal of copper (II) from aqueous solution using wheat straw-supported nanoscale zero-valent iron. Chem Eng J. 2020;379: 122384.
19. Hokkanen S, Bhatnagar A, Sillanpaa M. A review on modification methods to cellulose-based adsorbents to improve adsorption capacity. Water Res. 2016;91:156–73.
20. Atta NF, Galal A, Ali SM. The effect of the lanthanide ion-type in LnFeO3 on the Catalytic activity for the Hydrogen evolution in acidic medium. Int J Electrochem Sci. 2014;9:2132–48.
21. Ali SM, Al-Rahman YMA, Atta NF, Galal A. Catalytic activity of $LaBO_3$ for OER in $HClO_4$ medium: an approach to the molecular orbital theory. J Electrochem Soc. 2016;163:H81–8.
22. Ali SM, Al-Otaibi HM. The distinctive sensing performance of cobalt ion in $LaBO_3$ perovskite (B = Fe, Mn, Ni, or Cr) for hydrazine electrooxidation. J Electroanal Chem. 2019;851: 113443.
23. Eskandrani AA, Ali SM, Al-Otaibi HM. Study of the oxygen evolution reaction at strontium palladium perovskite electrocatalyst in acidic medium. Int J Mol Sci. 2020;21:3785.
24. Ali SM, Al Lehaibi HA. Smart perovskite sensors: the electrocatalytic activity of SrPdO3 for hydrazine oxidation. J Electrochem Soc. 2018;165:B345–50.
25. Zhou F, Ren Z, Zhao Y, Shen X, Wang A, Li YY, et al. Perovskite photovoltachromic supercapacitor with all-transparent electrodes. ACS Nano. 2016;10:5900–8.
26. Goel P, Sundriyal S, Shrivastav V, Mishra S, Dubal DP, Kim K. Perovskite materials as superior and powerful platforms for energy conversion and storage applications. Nano Energy. 2021;80: 105552.
27. Chang J, Chen H, Wang G, Wang B, Chen X, Yuan H. Electronic and optical properties of perovskite compounds $MA_{1-\alpha}FA_{\alpha}PbI_{3-\beta}X_{\beta}$ (X = Cl, Br) explored for photovoltaic applications. RSC Adv. 2019;9:7015–24.
28. Funabiki F, Toda Y, Hoson H. Optical and electrical properties of perovskite variant $(CH_3NH_3)_2SnI_6$. J Phys Chem C. 2018;122:10749–54.
29. Zhang D, Zhang CL, Zhou P. Preparation of porous nano-calcium titanate microspheres and its adsorption behavior for heavy metal ion in water. J Hazard Mater. 2011;186:971–7.
30. Ali SM, Eskandrani AA. The sorption performance of cetyl trimethyl ammonium bromide-capped $La_{0.9}Sr_{0.1}FeO_3$ perovskite for organic pollutants from industrial processes. Molecules. 2020;25:1640.
31. Haron W, Sirimahachai U, Wisitsoraat A, Wongnawa S. Removal of Cd^{2+} and Pb^{2+} from water by $LaGdO_3$ perovskite. SNRU J Sci Tech. 2017;9:544–51.
32. Ali SM, Al-Oufi B. Synergistic sorption capacity of $La_{0.9}Sr_{0.1}FeO_3$ perovskite for organic dyes by cellulose modification. Cellulose. 2020;27:429–40.

33. Ali SM, El Mansop MA, Galal A, Abd El-Wahab SM, El-Etr WMT, Zein El-Abdeen HA. Novel perovskite/biochar-based sorbent for removal of heavy metal ions: a correlation of the adsorption capacity with the metal ion characteristics. Sci Rep. 2023;13:9466.
34. Thakur M, Sharma A, Ahlawat V, Bhattacharya M, Goswami S. Process optimization for the production of cellulose nanocrystals from rice straw derived a-cellulose. Mat Sci Energy Tech. 2020;3:328–34.
35. Ali SM, Emran KM, Alrashedee FMM. Removal of organic pollutants by lanthanide-doped MIL-53 (Fe) metal-organic frameworks: effect of the dopant type in magnetite precursor. J Rare Earths. 2023;41:140–8.
36. Jiang W, Cheng L, Gao J, Zhang S, Wang H, Jin Z. Preparation of crystalline $LaFeO_3$ nanoparticles at low calcination temperature: precursor and synthesis parameter effects. Mater. 2021;14:5534.
37. Hamid S, Imane K, Djafer B. Thermal, structural and morphological studies of cellulose and cellulose nanofibers extracted from bitter watermelon of the cucurbitaceae family. J Polym Environ. 2020;28:1914–20.
38. Ngankam ES, Dai-Yang L, Debina B, Baçaoui A, Yaacoubi A, Rahman AN. Preparation and characterization of magnetic banana peels biochar for Fenton degradation of methylene blue. Mater Sci App. 2020;11:382–400.
39. Wang W, Liu P, Zhang M, Hu J, Xing F. The pore structure of phosphoaluminate cement. Open J Comp Mater. 2012;2:104–12.
40. Modak A, Bhanja P, Bhaumik A. Microporous nanotubes and nanospheres with iron-catechol sites: efficient lewis acid catalyst and support for Ag nanoparticles in CO2 fixation reaction. Chem Eur J. 2018;24:14189–97.
41. Ali SM, Galal A, Atta NF, Shammakh Y. Toxic heavy metal ions removal from wastewater by nano-magnetite: case study Nile river water. Egypt J Chem. 2017;60:601–12.
42. Ali SM, Emran KM, Al-Oufi ALL. Adsorption of organic pollutants by nano-conducting polymers composites: effect of the supporting nano-oxide type. J Mol Liq. 2017;233:89–99.
43. Kong Q, Preis S, Li L, Luo P, Wei C, Li Z. Relations between metal ion characteristics and adsorption performance of graphene oxide: a comprehensive experimental and theoretical study. Sep Purif Tech. 2020;232: 115956.
44. Zhao M, Dai Y, Zhang M, Feng C, Qin B, Zhang W. Mechanisms of Pb and/or Zn adsorption by different biochars: Biochar characteristics, stability, and binding energies. Sci Total Environ. 2020;717: 136894.
45. Ahmad Z, Gao B, Mosa A, Yu H, Yin X, Bashir A. Removal of Cu (II), Cd (II) and Pb (II) ions from aqueous solutions by biochars derived from potassium-rich biomass. J Clean Prod. 2018;180:437–49.

Publisher's Note